Mathematical Simulation on Solid Flow in COREX Melter Gasifier Using Discrete Element Method

Han Lihao[1*], Li Yuehua[2], Liu Yanxia[1], Huang Weiqing[1], Qi Suci[1], Guan Xin[1]

[1] Material Engineering Department, Hebei College of Industry and Technology, Shijiazhuang, 050091, P. R. China.

[2] Basic Course Teaching Department, Hebei College of Industry and Technology, Shijiazhuang, 050091, P. R. China.

* Corresponding author. Email: 2773298420@qq.com

Manuscript submitted June 12, 2019; accepted August 8, 2019.
doi: 10.17706/ijapm.2019.9.4.196-204

Abstract: Based on the principle of discrete element method (DEM), a 2D slot model of COREX melter gasifier has been established to analyze the solid flow pattern, velocity field and porosity distribution at a microscopic level. The results show that the solid flow pattern changes from linear mode to curving down on the both sides by means of joining tracer particles, which states that the descending velocity near the furnace wall is higher than the velocity near the furnace center. The results also confirm that the solid flow can be divided into several different flow zones including dead zone where the velocity of particle is low or motionless, the plug flow zone where the velocity distribution is uniform, and the channel flow zone which is located between the dead zone and the plug flow zone. The velocity distribution is asymmetric showing that there exits segregation phenomenon in the furnace, and the porosity distribution also clarifies this phenomenon. The influence of raceway in the vertical direction is limited to the region of 0.18 m from the hearth bottom level. The decrease of raceway size causes that the active region with higher velocity becomes shrink and the height of dead zone increases remarkable. The porosity is 0.37 in the dead zone, while in the raceway the porosity is 0.65, the porosity in the plug flow zone is between 0.37 and 0.65, and the porosity of upper free space is about 1.

Key words: COREX melter gasifier, discrete element method, porosity distribution, solid flow pattern.

1. Introduction

Melter gasifier, which is the key device of COREX process, has been mainly used for coal gasification, heat supply, melting of pre-reduced ore, final reduction and carburization of molten iron and so on. It is similar to the blast furnace(BF) that is also a gas-solid counter-current reactor. Direct reduction iron (DRI) and coal (coke) particles are mixing charged from the upper of melter gasifier, and the pure oxygen with room temperature is blown from tuyeres. DRI particles are reduced during descending and many physical changes and chemical reactions between each phase are undergoing in there. Its stable operation is closely related with the smoothly descending of burden. The terrible phenomenon like tunnel and hanging will happen once the normal descending condition is broken. Thus, it is necessary to study the burden behavior in the COREX melter gasifier.

Currently, it is in lack of researches related to solid flow in COREX melter gasifier so far due to the dominant role of BF in hot metal producing. Therefore, the present literature studies were inspired on the

basis of adequate and developed studies on BF solid flow behaviors. There have been three approaches adopted for providing some means of studying the solid flow behaviors of BF-physical modeling [1]-[4], continuous fluid model based on the particle dynamic and DEM. Takahashi *et al*. [5] obtained the flow pattern that the particle flowing into raceway and deadman using a cold model. It is shown that there are three characteristic flow regions including smoothly main stream, deadman with particle motionless and quasi stagnant zone. Zhang *et al*. [6] studied the formation of deadman and solid flow behaviors adopting continuous mechanics method. Recently, with the development of computer technology, the discrete element method which occupies large computer memory attracts the attention of lots of scholars [7]-[10]. The discrete element method which is originally developed by Cundall and Strack [11] has been applied in many fields, such as process engineering, mining and geology and so on. It is the representative method that simulates the discontinuous media. In this paper, based on the principle of DEM, a 2D slot model of COREX melter gasifier has been established. Using the proposed model, the solid flow pattern, velocity field and porosity distribution was analyzed at a microscopic level.

2. Mathematical Model

2.1. Introduction of Simulation Method

DEM [11] started relatively late in China, and its originally research subjects are mainly focus on the mechanical behaviors such as rock and discontinuous media. The interaction force between two particles represented by spring-damper-friction plate is shown in Fig. 1. The particle *i* bears two kinds of forces which are gravity $m_i\mathbf{g}$ and the contact force between particle and particle, as well as particle and wall. In addition, the particle *i* bear two kinds of torques which are tangential torque and rolling friction torque. Based on the Newton's second law of motion, the governing equations for the translational and rotational motion of particle *i* can be written as

$$m_i\left(\mathrm{d}\boldsymbol{v}_i\right)/\mathrm{d}t = \sum_{\mathrm{j}=1}^{\mathrm{k_i}}(\boldsymbol{F}_{\mathrm{cn},ij} + \boldsymbol{F}_{\mathrm{dn},ij} + \boldsymbol{F}_{\mathrm{ct},ij} + \boldsymbol{F}_{\mathrm{dt},ij}) + m_i\mathbf{g} \tag{1}$$

$$\boldsymbol{I}_i\, d\boldsymbol{\omega}_i/dt = \sum_{j=1}^{k_i}\left(\boldsymbol{T}_{ij} + \boldsymbol{M}_{ij}\right) \tag{2}$$

where, m_i, $\boldsymbol{I}_i$, $\mathbf{v}_i$, $\boldsymbol{\omega}_i$ represent mass, rotational inertia, translational velocity and rotational velocity of particle *i*, respectively. $m_i\mathbf{g}$ represents the gravity of particle *i*. $\boldsymbol{F}_{\mathrm{cn},ij}$, $\boldsymbol{F}_{\mathrm{ct},ij}$, $\boldsymbol{F}_{\mathrm{dn},ij}$, $\boldsymbol{F}_{\mathrm{dt},ij}$, $\boldsymbol{T}_{ij}$, $\boldsymbol{M}_{ij}$ represent the normal and tangential contact force, normal and tangential damp force, tangential and rolling friction torque acting on *i*, respectively. k_i denotes the particle numbers contacting with particle *i*. Based on the previous literature [12], the equations of contact force, damping force, friction force and torque are listed in Table 1.

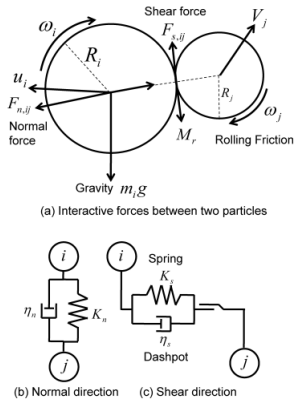

Fig. 1. Depiction of interaction forces between two particles.

Table 1. Components of Forces and Torques Acting on Particle *i*

Force and Torque		*Symbol*	*Equation*
Normal	Contact force	$\mathbf{F}_{\mathrm{cn},ij}$	$-4/3E^{*}\sqrt{R^{*}}\delta_{\mathrm{n}}^{3/2}\hat{\mathbf{n}}$
	Damping force	$\mathbf{F}_{\mathrm{dn},ij}$	$-c_{\mathrm{n}}(6m_{ij}E^{*}\sqrt{R^{*}\delta_{\mathrm{n}}})^{1/2}\mathbf{v}_{\mathbf{n},ij}$
Tangential	Contact force	$\mathbf{F}_{\mathrm{ct},ij}$	$-\mu_{\mathrm{s}}\lvert\mathbf{F}_{\mathrm{cn},ij}\rvert(1-(1-\delta_{\mathrm{t},ij}/\delta_{\mathrm{t},ij,\max})^{3/2})\hat{\boldsymbol{\delta}}_{\mathrm{t}}\quad(\delta_{\mathrm{t},ij}<\delta_{\mathrm{t},ij,\max})$
	Damping force	$\mathbf{F}_{\mathrm{dt},ij}$	$-c_{\mathrm{t}}(6\mu_{\mathrm{s}}m_{ij}\lvert\mathbf{F}_{\mathrm{cn},ij}\rvert\sqrt{1-\delta_{\mathrm{t},ij}/\delta_{\mathrm{t},ij,\max}}/\delta_{\mathrm{t},ij,\max})^{1/2}\mathbf{v}_{\mathrm{t},ij}$ $(\delta_{\mathrm{t},ij}<\delta_{\mathrm{t},ij,\max})$
Friction force		$\mathbf{F}_{\mathrm{t},ij}$	$-\mu_{\mathrm{s}}\lvert\mathbf{F}_{\mathrm{cn},ij}\rvert\hat{\boldsymbol{\delta}}_{\mathrm{t}}(\delta_{\mathrm{t},ij}>\delta_{\mathrm{t},ij,\max})$
Gravity		$\mathbf{F}_{\mathrm{g}i}$	$m_i\mathbf{g}$
Tangential torque		$\mathbf{T}_{\mathrm{t},ij}$	$\mathbf{R}_{ij}\times(F_{\mathrm{ct},ij}+F_{\mathrm{dt},ij})$
Rolling friction torque		$\mathbf{M}_{\mathrm{r},ij}$	$\mu_{\mathrm{r},ij}\lvert F_{\mathrm{cn},ij}\rvert\hat{\boldsymbol{\omega}}_{\mathrm{t},ij}^{\mathrm{n}}$

where, $\frac{1}{R^{*}}=\frac{1}{\lvert\mathbf{R}_i\rvert}+\frac{1}{\lvert\mathbf{R}_j\rvert}$, $E^{*}=\frac{E}{2(1-\nu^2)}$, $\hat{\mathbf{n}}=\frac{\mathbf{R}_i}{\lvert\mathbf{R}_i\rvert}$, $\hat{\boldsymbol{\omega}}_{t,ij}=\frac{\boldsymbol{\omega}_{t,ij}}{\lvert\boldsymbol{\omega}_{t,ij}\rvert}$, $\hat{\boldsymbol{\delta}}_t=\frac{\boldsymbol{\delta}_t}{\lvert\boldsymbol{\delta}_t\rvert}$, $\delta_{\mathrm{t},ij,\max}=\mu_{\mathrm{s}}\frac{2-\nu}{2(1-\nu)}\delta_{\mathrm{n}}$,

$\mathbf{v}_{ij}=\mathbf{v}_j-\mathbf{v}_i+\boldsymbol{\omega}_j\times\mathbf{R}_j-\boldsymbol{\omega}_i\times\mathbf{R}_i$, $\mathbf{v}_{\mathrm{n},ij}=(\mathbf{v}_{ij}\cdot\hat{\mathbf{n}})\hat{\mathbf{n}}$, $\mathbf{v}_{\mathrm{t},ij}=\mathbf{v}_{ij}-\mathbf{v}_{\mathrm{n},ij}$

Porosity is an important physical parameter that expresses the microscopic structure of packing bed. It is related to particle physical property and packing state, as well as the motion of particles. Considering the porosity of packed bed has an important influence on the gas flow distribution of melter gasifier, a method to calculate porosity [13] has been introduced in this paper. Porosity is represented with the void volume divided by the cell volume. The porosity is obtained indirectly by calculating the volume of particles in the computational cell, which is given in (3), as shown in Fig. 2.

$$\varepsilon=1-\frac{\sum_{i=1}^{N}V_i}{\Delta V} \tag{3}$$

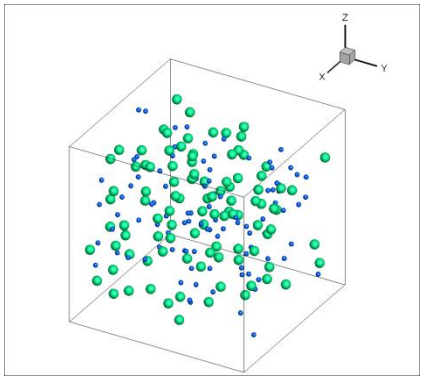

Fig. 2. Calculation method of porosity.

2.2. Simulation Conditions

The number of burden particles in the COREX melter gasifier is much larger than capable number for handling by the present discrete element method. Fig. 3 shows the computation geometry which is the same as the experiment device used by Zhou [14]. Larger particle size and higher discharging velocity are

used in the simulation in order to reduce the computation time. The simulation is started with the random generation of certain number of uniform spheres without overlaps, followed by a gravitational settling process for 2.5 s. Then the particles are discharged at a preset rate from the raceway region and added back to the top of the model of melter gasifier to maintain the macroscopic steady flow as the case in an actual melter gasifier. Fig. 4 shows the initial packing state. The size of random generation region is 0.440 mm×100 mm×100 mm, as shown in the upper part of Fig. 3.

The raceway is assumed as spherical shape with 30 mm in radius. The particles entrained the raceway area are uniformly vanished at a set interval. The packed bed height is 420 mm. The material properties in the simulation are listed in Table 2.

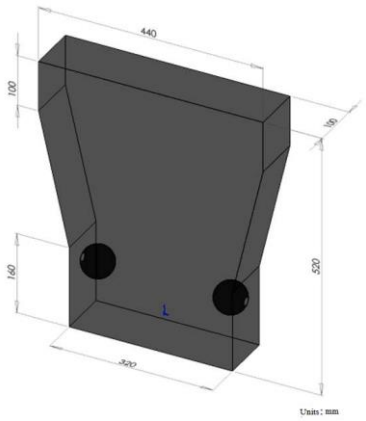

Fig. 3. Computation geometry.

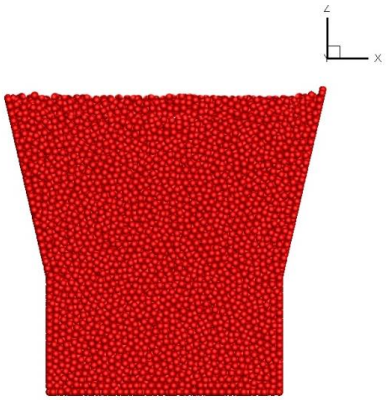

Fig. 4. Initial packing state in 2D slot model.

3. Results and Discussions

3.1. Solid Flow Pattern and Velocity Field

To understand the solid flow in melter gasifier in detail where the mixed charging pattern is adopted, the method joining tracer particles is employed. Fig. 5 shows the solid flow pattern with single tracer particles layer.

Fig. 5(a) shows the initial packing state with tracer particles, at this moment, the discharging starts. Firstly, the tracer particles layer initially shows as linear mode. As time goes on, the layer becomes decurved near the side wall. It is shown that the descending velocity near the side wall is higher than the velocity near the furnace center because of the laboratory-scale melter gasifier having two orifices near the side wall.

Table 2. Simulation Parameters

Variables	*Value*
Particle shape	Sphere
Particle number, N(-)	16000
Particle density, ρ_p(kg·m^{-3})	1100/1200
Particle diameter, d_p(mm)	10
Particle-particle sliding frictional coefficient, $\mu_{s,pp}$	0.5
Particle-particle rolling frictional coefficient, $\mu_{s,pp}$	0.0005
Particle-wall sliding frictional coefficient, $\mu_{r,pw}$	0.5
Particle-wall rolling frictional coefficient, $\mu_{r,pw}$	0.0005
Young's modulus of particle, E_p(Pa)	2160000
Young's modulus of wall, E_w(Pa)	2160000
Poisson's ratio of particle, ν_p	0.3
Poisson's ratio of wall, ν_w	0.3
Time step, $\triangle t$(s)	5.0×10^{-5}

**It is assumed that the walls have the same properties as the particles in this paper.

Fig. 6 shows the calculated particle velocity distributions in the vertical section at certain interval times. Fig. 6(a) shows the initial packing state of burden, and it is obviously shown that the particle velocity is almost zero. Then, the discharging process starts. What can be seen from Fig. 6(b) to (f) is that there are several different flow zones: dead zone located in the lower part of the furnace where the velocity of particle is low or motionless, the plug flow located in the upper part of the furnace where the velocity distribution is uniform, and the channel flow located between dead zone and plug flow zone. It can be also seen that although the position of raceway is symmetry, the velocity distribution is asymmetric which shows that there exits segregation phenomenon in the furnace.

Fig. 7 shows the calculated particle velocity distributions in the vertical section and the horizontal cross sections at 0-0.06 m, 0.06-0.12 m, 0.12-0.18 m, 0.18-0.24 m, 0.24-0.30 m and 0.30-0.36 m over the hearth bottom level, respectively. The active particles with higher velocity are concentrated in the upper part of raceway. The influence of the raceway in the horizontal cross section can be clearly observed in the range of 0.08 m from the wall at 0-0.06 m and 0.06-0.12 m over the hearth bottom level. Totally, the velocity difference across the horizontal cross section can be recognized especially within 0.18 m over the hearth bottom level. In the case of (d), namely, at 0.18-0.24 m level over the hearth bottom level, the velocity of particles are distributed almost uniformly in the horizontal section compared with (a) (b) and (c).

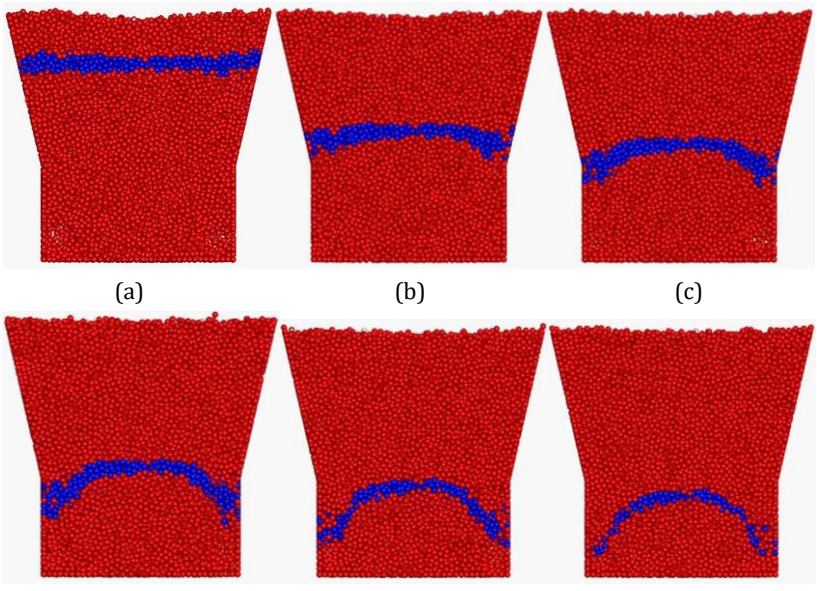

(a) (b) (c)

(d) (e) (f)

Fig. 5. Solid flow pattern of joining tracer particles layer.

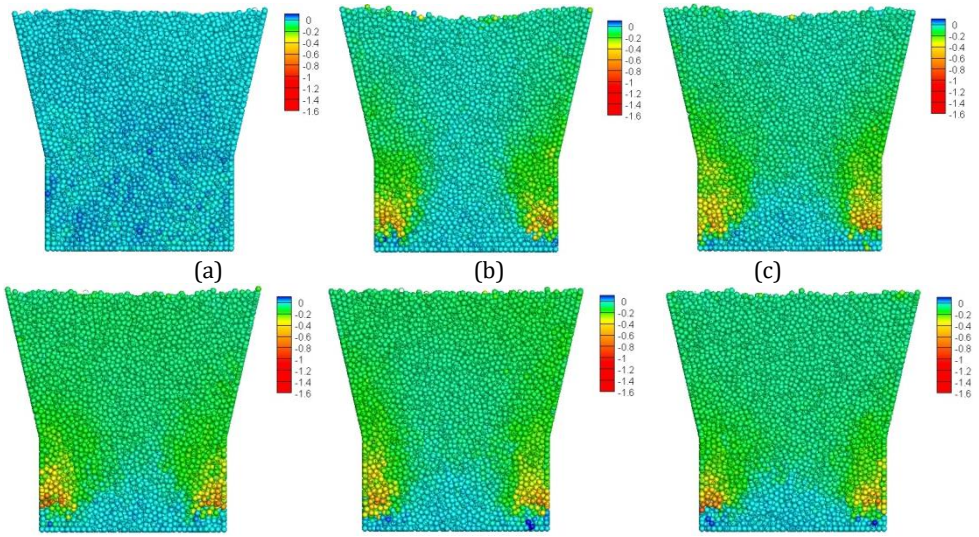

Fig. 6. Velocity distributions in 2D slot model (m/s).

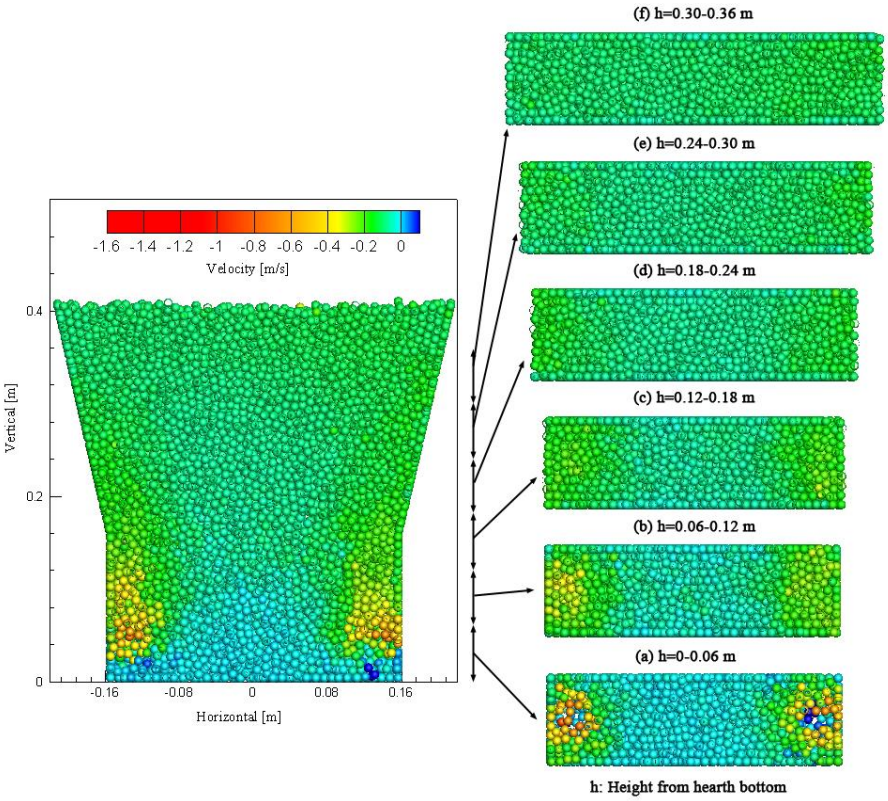

Fig. 7. Velocity distribution of particles in the vertical and horizontal sections with raceway radius 0.03 m.

3.2. Porosity Distribution

The porosity is also related to the permeability of the packed bed, and it is one of the critical factors to stabilize the operation and smooth of melter gasifier. Therefore, it is very necessary to study the porosity distribution.

Fig. 8 shows the porosity distribution of the whole furnace. It is seen that the porosity is 0.37 in the dead zone, while in the raceway the porosity is about 0.65, the porosity in the plug flow zone is between 0.37 and 0.65, and the porosity of upper free space is 1. These porosity data can provide basis for calculating the gas

distribution in melter gasifier. It is also seen that the solid flow is asymmetrical in the furnace.

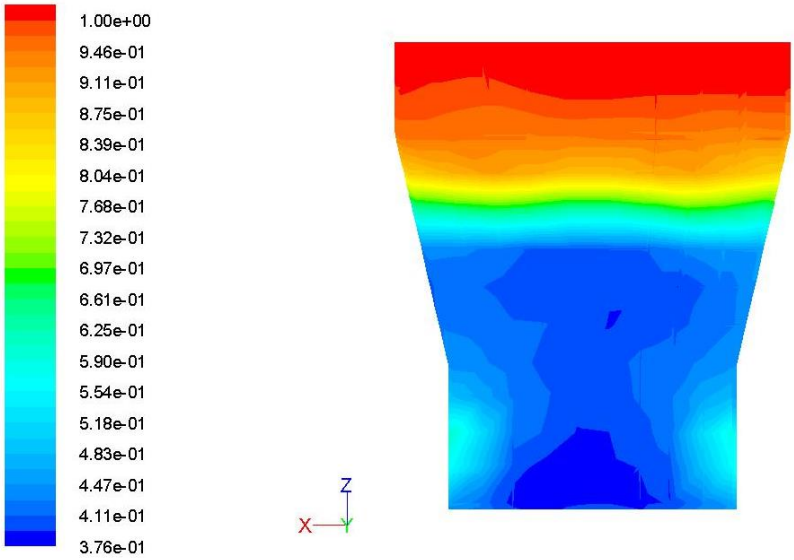

Fig. 8. Porosity distribution in the 2D slot model.

3.3. Influence of Raceway Size on Velocity Field

This paper also presents the influence of raceway size on velocity field. Fig. 9 shows the calculated particle velocity distributions in the vertical section and the horizontal cross sections with the raceway radius of 0.02 m. The region of dead zone with stagnant particles becomes larger with the decrease of the raceway size. Compared with the reference condition shown in Fig. 7, the region with higher velocity on the upper side of raceway becomes narrow. The nonuniform distribution of velocity of particles in horizontal direction is not obvious. Since decreasing raceway size causes decreasing the active area, therefore, the region of dead zone increases in the height.

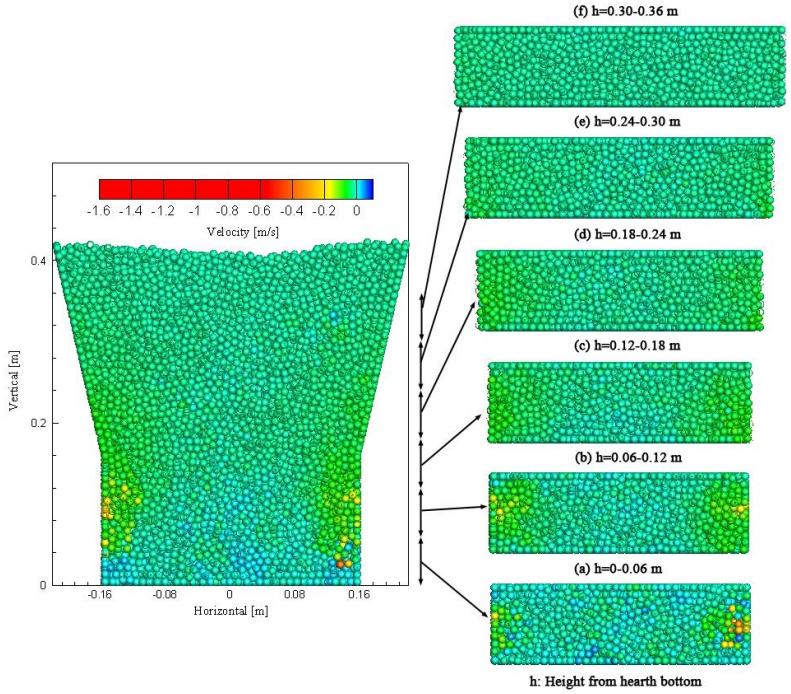

Fig. 9. Velocity distribution of particles in the vertical and horizontal sections with raceway radius 0.02 m.

4. Conclusions

Based on the principle of DEM, a 2D slot model of COREX melter gasifier has been established. The solid flow pattern, velocity field and porosity distribution were analyzed by using the proposed model at a microscopic level. The following results were obtained.

1) The solid flow pattern was analyzed through joining tracer particles. As the discharging process goes on, the solid flow pattern changes from linear mode to curving down on the both sides.
2) The solid flow can be divided into several different flow zones: dead zone where the velocity of particles is low or motionless, the plug flow zone where the velocity distribution is uniform, and the channel flow zone which is located between dead zone and plug flow zone. Although the position of raceway is symmetry in the present model, the velocity distribution is asymmetric which shows that there exits segregation phenomenon in the furnace. The porosity distribution also clarifies this phenomenon.
3) The influence of raceway in the vertical direction is limited to the region of 0.18 m from the hearth bottom level. With the decrease of raceway size, the active area decreases and the region of dead zone increases in the height.
4) The porosity distribution is as follows. The porosity is 0.37 in the dead zone, while in the raceway the porosity is about 0.65, the porosity in the plug flow zone is between 0.37 and 0.65, and the porosity of upper free space is 1. These porosity data can provide basis for calculating the gas distribution in melter gasifier.

Totally, by the application of DEM, the solid flow pattern which cannot be directly observed in the actual COREX melter gasifier can be simulated expediently. It has a promising prospect in better understanding the solid flow of COREX melter gasifier in the future, i.e. considering cohesive zone, liquid and gas etc.

Conflict of Interest

The authors declare no conflict of interest.

Author Contributions

Han Lihao conducted the research; Li Yuehua analyzed the data; Liu Yanxia wrote the paper; Huang Weiqing also analyzed the data and processed the figures; Qi Suci consulted relevant literatures; Guan Xin wrote the DEM programme; all authors had approved the final version.

Acknowledgment

This project is supported by Scientific Research Fund of Hebei College of Industry and Technology, and yet supported by the Natural Science Foundation of Hebei Province (E2017417008).

References

[1] Takahashi, H., & Komatsu, N. (1993). *ISIJ Int* (vol. 33, p. 655).
[2] Nozawa, K., Kamijo, T., & Shimizu, M. (1995). *Tetsu-to-Hagané* (vol. 81, p. 882).
[3] Takahashi, H., *et al*. (2007). *Tetsu-to-Hagané* (vol. 93, p. 615).
[4] Matsui, Y., *et al*. (2006). *Tetsu-to-Hagané* (vol. 92, p. 932).
[5] Takahashi, H., *et al*. (2005). *ISIJ Int* (vol. 45, p. 1386).
[6] Zhang, S. J., *et al*. (1998). *ISIJ Int* (vol. 38, p. 1311).
[7] Adema, A. T., *et al*. (2010). *ISIJ Int* (vol. 50, p. 954).
[8] Wang, Y. J., & Tao, L. J. (1997). *Journal of Northeastern University: Natural Science* (vol. 18, p. 374).
[9] Fan, Z. Y., *et al*. (2010). *ISIJ Int* (vol. 50, p. 1406).

[10] Kim, S. Y., & Sasaki, Y. (2010). *ISIJ Int* (vol. 50, p. 813).
[11] Cundall, P. A., & Strack O. D. L. (1979). *Geotechnique* (vol. 29, p. 47).
[12] Zhu, H. P., *et al*. (2007). *Chemical Engineering Science* (vol. 62, p. 3378).
[13] Li, H. F., *et al*. (2012). *Journal of iron and steel research, International* (vol. 19, p. 36).
[14] Zhou, X. L., *et al*. (2011). *Advanced Materials Research* (vol. 284-286, p. 1184).

Han Lihao is doctor, lecturer of ferrous metallurgy. He graduated from the Northeastern University in 2015. He worked in Hebei College of Industry and Technology. His research interests include non-blast furnace and blast furnace.

Li Yuehua is master of English language and literature. She graduated from the Northeastern University in 2014. She worked in Hebei College of industry and technology. Her research interests include English language and literature.

Liu Yanxia is associate professor of ferrous metallurgy. She graduated from the Inner Mongolia University of Science&Technology in 2006. She worked in Hebei College of Industry and Technology. Her research interests include sinter and ironmaking process.

Huang Weiqing is associate professor of ferrous metallurgy. She graduated from the Northeastern University in 2006. She worked in Hebei College of Industry and Technology. Her research interests include ironmaking and BOF.

Qi Suci is associate professor of ferrous metallurgy. She graduated from the Inner Mongolia University of Science&Technology in 2006. She worked in Hebei College of Industry and Technology. Her research interests include metallurgical equipment and ironmaking process.

Guan Xin is associate professor of materials science. She graduated from the Hebei University of Technology in 2000. She worked in Hebei College of Industry and Technology. Her research interests include metallurgical equipment, materials science and material preparation.